Using an ultra-thin non-doped orange emission layer to realize high efficiency white organic light-emitting diodes with low efficiency roll-off

Liping Zhu, Yongbiao Zhao, Hongmei Zhang, Jiangshan Chen, and Dongge Ma

Citation: Journal of Applied Physics **115**, 244512 (2014); doi: 10.1063/1.4886179
View online: http://dx.doi.org/10.1063/1.4886179
View Table of Contents: http://scitation.aip.org/content/aip/journal/jap/115/24?ver=pdfcov
Published by the AIP Publishing

Using an ultra-thin non-doped orange emission layer to realize high efficiency white organic light-emitting diodes with low efficiency roll-off

Liping Zhu,[1] Yongbiao Zhao,[2] Hongmei Zhang,[3] Jiangshan Chen,[1] and Dongge Ma[1,a)]
[1]*State Key Laboratory of Polymer Physics and Chemistry, Changchun Institute of Applied Chemistry, Chinese Academy of Sciences, Graduate University of the Chinese Academy of Sciences, Changchun 130022, People's Republic of China*
[2]*Luminous! Center of Excellence for Semiconductor Lighting and Displays, School of Electrical and Electronic Engineering, Nanyang Technological University, 50 Nanyang Avenue, Singapore, Singapore 639798*
[3]*Department of Materials Science and Engineering, Nanjing University of Posts and Telecommunications, Nanjing 210023, People's Republic of China*

(Received 6 April 2014; accepted 19 June 2014; published online 30 June 2014)

By adopting an ultra-thin non-doped orange emission layer sandwiched between two blue emission layers, high efficiency white organic light-emitting diodes (WOLEDs) with reduced efficiency roll-off were fabricated. The optimized devices show a balanced white emission with Internationale de L'Eclairage of (0.41, 0.44) at the luminance of 1000 cd/m^2, and the maximum power efficiency, current efficiency (CE), and external quantum efficiency reach 63.2 lm/W, 59.3 cd/A, and 23.1%, which slightly shift to 53.4 lm/W, 57.1 cd/A, and 22.2% at 1000 cd/m^2, respectively, showing low efficiency roll-off. Detailed investigations on the recombination zone and the transient electroluminescence (EL) clearly reveal the EL processes of the ultra-thin non-doped orange emission layer in WOLEDs.
 [http://dx.doi.org/10.1063/1.4886179]

I. INTRODUCTION

Recently, white organic light-emitting diodes (WOLEDs) have been receiving extensive attention in both research and industry by their capability to emit white light with high efficiency and to be applied to color displays and solid state lighting owning to the unique features of organic semiconducting materials such as flexibility over large area, low cost fabrication, and tunable colors.[1–5] To maximize the intrinsic efficiencies of WOLEDs, phosphorescent molecules are often used as emitters, which allow for efficient light emission from both excited singlet and triplet states and can lead to a nearly 100% internal quantum efficiency (IQE) compared with fluorescent materials (25%).[6] Therefore, all phosphorescent WOLEDs often show higher performance than the fluorescent counterparts. In the fabrication of high efficiency phosphorescent OLEDs, it is necessary to generally dope phosphorescence dyes into relative host by proper concentration in order to suppress the efficiency degradation caused by concentration quenching as well as to make the full use of the generated excitons.[1] As we know, the utilization of complementary colors or three primary colors is necessary to realize the white emission. Up to now, several emission layer (EML) structures have been proposed to fabricate high efficiency phosphorescent WOLEDs such as multilayer structures consisted of respective red, green, and blue doped emission layers,[4,7–12] and single-layer structures by doping red, green, and blue dyes in single host.[13–15] It can be seen that either the multilayer structures or the single-layer structures are complicated in processing technique, where the emissive layer sequence in multilayer and doping concentration in single-layer have to accurately control and the white emission color often exhibits strong change with the applied voltages in doping single-layer structure.[13] Therefore, further simplifying the device structures but yet realizing high efficiency has been a trend in the fabrication of WOLEDs. Comparatively, by introducing an ultra-thin non-doping phosphorescent dye layer within the EML seems a simple and effective method for WOLEDs,[16–21] where not only the processing is greatly simplified but also the high efficiency can be well realized. For example, Lee *et al.*[21] has demonstrated a WOLED by dispersing an ultra-thin host-free, yellow phosphorescent layer in between double blue phosphorescent emitters. The device exhibited a power efficiency (PE) of 35 lm/W at the brightness of 1000 cd/m^2, which is a comparable value to that of using a complicated host-guest doping system to realize the yellow emission in WOLEDs. Zhao *et al.*[20] has fabricated two colors, three colors, and four colors WOLEDs by using the ultra-thin non-doped emissive layer method. Here, they introduced thin non-doped red, yellow, green, and blue emission layers into the hole transport layer in proper position and at the interface between hole transport layer and electron transport layer to realize the white emission. The power efficiencies of 37 lm/W, 29 lm/W, and 19 lm/W at brightness of 1000 cd/m^2 for the two-color, three-color, and four-color WOLEDs, respectively, have been well obtained. However, it is clearly seen that the power efficiency of WOLEDs based on the ultra-thin non-doped emissive layer concept is far from the requirement of practical lighting applications and lower than the traditional WOLEDs,[4,22] which is urgent to further improve, and its emission mechanism and effect factors are also necessary to deeply understand and elucidate.

In order to simplify the structure of WOLED as well as to maintain the high efficiency, in this paper, we fabricated

a)Author to whom correspondence should be addressed. Electronic mail: mdg1014@ciac.ac.cn. Tel.: +86 431 85262357. Fax: +86 43185262873.

high power efficiency two-color all phosphorescence WOLEDs by simply inserting an ultra-thin non-doped orange emission layer in between two doped blue emission layers. It can be found experimentally that the optimized devices show a good white emission and high efficiency with near 100% internal quantum efficiency and low roll-off, fully indicating the advantage of the simple and cost-saved ultra-thin non-doped emissive layer method on constructing high efficiency WOLEDs. Furthermore, by examining the exciton density through the EML, the reason for the high efficiency is revealed.

II. EXPERIMENTAL

All the devices were fabricated on glass substrates pre-coated with 180 nm indium tin oxide (ITO) with a sheet resistance of 10 Ω/sq. The ITO substrates were degreased in ultrasonic solvent bath and then dried at 120 °C for 30 min. Before loaded into the deposition chamber, the ITO surface was treated with UV-ozone for 15 min. All the layers were grown by thermal evaporation in a high-vacuum system with a pressure of less than 5×10^{-4} Pa without breaking vacuum. The various device structures were described in the text. The organics and metal oxide were evaporated at the rate in a range of 1–2 Å/s except that the evaporation rate of ultra-thin layer is 0.02 Å/s, and the metals were evaporated at the rate of 8–10 Å/s. The overlap between ITO and Al electrodes was 4 mm × 4 mm, which is the active emissive area of the devices. The current–voltage–brightness characteristics were measured by using a set of Keithley source measurement units (Keithley 2400 and Keithley 2000) with a calibrated silicon photodiode. The electroluminescence (EL) spectra were measured by a Spectrascan PR650 spectrophotometer. All the measurements were carried out in ambient atmosphere at room temperature.

For the transient electroluminescence measurements, the devices were electrically excited by a pulse generator (Agilent 8114 A, 100 V/2 A) with a duration of 10 μs, and the transient EL signals pass through a monochromator and collected by a photomultiplier tube (PMT). The results were then displayed on an oscilloscope (Agilent Model 54825A, 500 MHz/2 GSa/s). The EL lifetime was obtained by a single exponential fit of emission decay curves.

III. RESULTS AND DISCUSSION

The fabricated WOLED structure was ITO/MoO_3 (10 nm)/1,1′-bis[4–(di-*p*-tolylamino)phenyl]cyclohexane (TAPC): MoO_3 (20%, 50 nm)/TAPC (30 nm)/4,4′,4″-tri(*N*-carbazolyl) triphenylamine (TCTA): bis(3,5-difluoro-2–(2-pyridyl)phenyl-(2-carboxypyridyl))iridium III (FIrpic) (10%, 5 nm)/bis(2-phenyl-benzothiozolato-N,$C^{2'}$)iridium(acetylacetonate) ($Ir(bt)_2(acac)$) (x nm)/2,6-bis(3–(carbazol-9-yl)phenyl)pyridine (26DCzPPy): FIrpic (20%, 5 nm)/1,3-bis(3,5-dipyrid-3-yl-phenyl)benzene (BmPyPB) (10 nm)/BmPyPB: Li_2CO_3 (3%, 30 nm)/Li_2CO_3 (1 nm)/Al (100 nm), where x = 0.02, 0.04, 0.06, and 0.08 nm, respectively, as shown in Figure 1(a). The chemical structures of the involved materials are depicted in Figure 1(b). Here, TAPC and BmPyPB are served as effective carrier (hole and electron) transport layers and exciton blocking layers. The double blue layers are composed of 10% FIrpic doped TCTA and 20% FIrpic doped 26DCzPPy. The thickness of $Ir(bt)_2(acac)$ is increased from 0.02 nm to 0.08 nm in order to adjust the ratio of blue emission to orange emission in the white spectra. Figure 2(a) shows the current density-voltage-luminance (*J-V-L*) characteristics of the resulting devices. The *J-V* curves are almost independent on the varied thickness of orange emission layer, suggesting that the change of the orange emission layer will not affect the transport properties in the devices. And in the *L-V* curves, the device with 0.02 nm orange layer shows slightly lower luminance than the other three devices, which might be originated from the emission saturation of orange dye due to thin orange layer. Table I summarizes the CE (current

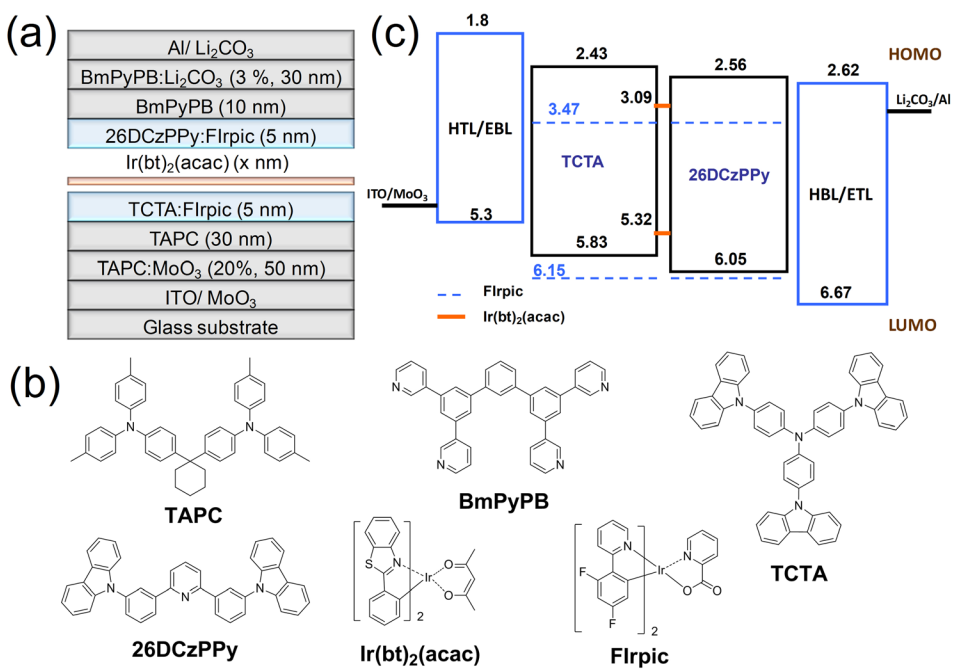

FIG. 1. (a) Structure of the resulting WOLEDs. (b) Chemical structures of the materials used in this study. (c) Proposed energy diagram of the device.

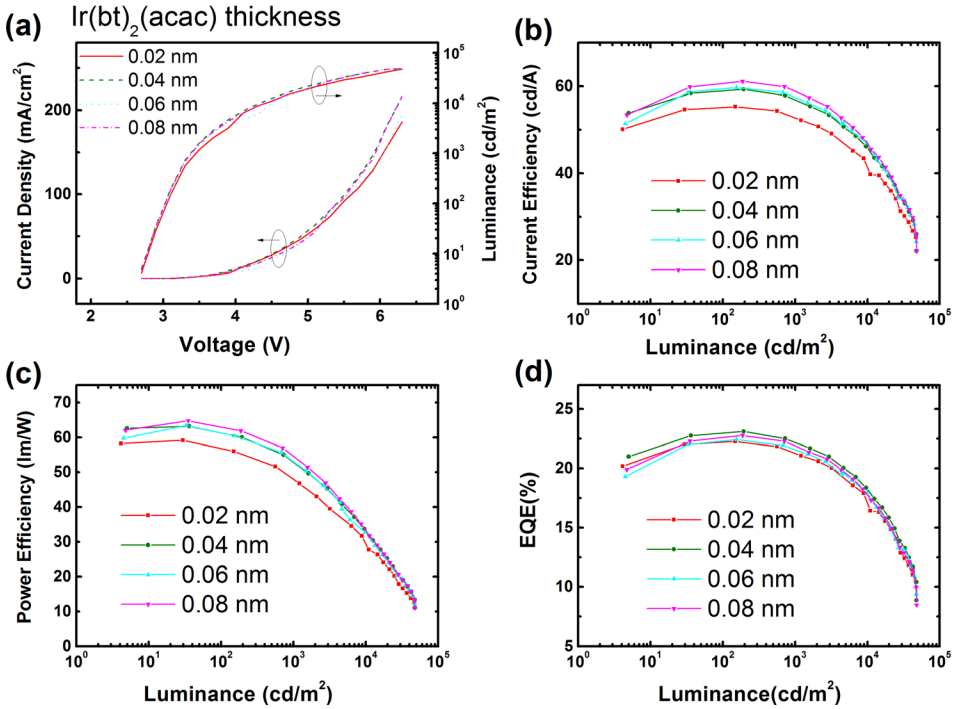

FIG. 2. EL performance of the resulting WOLEDs. (a) Current density-voltage-luminance characteristics of devices with varied thicknesses of $Ir(bt)_2(acac)$. (b) Current efficiency, (c) power efficiency, and (d) external quantum efficiency as a function of luminance at different thicknesses of 0.02 nm (square), 0.04 nm (circle), 0.06 nm (up triangle), and 0.08 nm (down triangle).

efficiency, cd/A), PE (lm/W), and EQE (external quantum efficiency, %. EQE = IQE*η_{out}, here IQE is defined as the internal quantum efficiency, η_{out} is the out-coupling efficiency) characteristics of the devices from Figure 2. All the devices show turn-on voltage of 2.7 V, which is as low as the triplet energy gap ($T_1 \sim 2.62$ eV) of phosphorescent dopant, FIrpic. The four devices show maximum EQE of 22.3%, 23.1%, 22.4%, and 22.3%, respectively, which indicate that the IQE is nearly 100% if the out-coupling efficiency is about 20%–30%. From the slightly increasing orange emission layer thickness from 0.02 nm to 0.08 nm, PE and CE increase gradually from 48.4 lm/W to 55.1 lm/W and 52.9 cd/A to 59.1 cd/A at 1000 cd/m^2, respectively. It is our best known that this performance should be the best results among state-of-the-art complementary color WOLEDs.

The EL spectra of these four devices at different luminances are shown in Figure 3. It is clearly seen that they all show excellent white emission, and the orange emission increases with increasing the orange emission layer thickness. Obviously, the orange emission at 560 nm peak and 600 nm shoulder is originated from $Ir(bt)_2(acac)$, while the blue emission centered at 472 nm is originated from FIrpic. The four devices show, respectively, Internationale de L'Eclairage (CIE) of (0.31, 0.40), (0.35, 0.42), (0.41, 0.44), and (0.42, 0.45) at the luminance of 1000 cd/m^2. The relative intensity of orange emission to blue emission decreases with the increase of luminance, which is probably due to the creation of more triplet excitons on FIrpic with the voltages,[23] or the saturation of emission from $Ir(bt)_2(acac)$ molecules.

For the resulting WOLEDs based on ultra-thin non-doped orange emission layer, the control of exciton recombination zone (RZ) position is obviously very important. The fact that the orange emission from $Ir(bt)_2(acac)$ and the blue emission from FIrpic are simultaneously obtained in our WOLEDs, as shown in Figure 3, indicates that the exciton recombination zone should be localized in the region at the interface between TCTA:FIrpic and 26DCzPPy:FIrpic layers. In order to evaluate the concrete position of recombination zone and the possible exciton density distribution in EML, we fabricated OLEDs based on the same structure as the resulting WOLEDs only by changing the position of a 0.06 nm $Ir(bt)_2(acac)$ thin layer in TCTA:FIrpic/26DCzPPy:FIrpic EML. Thus, a series of spectra of varied orange layer positions were obtained. Figure 4 plots the ratio of the orange emission peak intensity to the blue intensity as a function of the position of orange thin layer at a driving voltage of 3.9 V. The position at the interface between TCTA:FIrpic and 26DCzPPy:FIrpic layers is set to zero. It is clearly that the strongest orange emission can be obtained as the thin orange layer is posited at the interface between TCTA:FIrpic

TABLE I. Summary of the EL performance of the WOLEDs with different thicknesses of orange emission layer. Here, CRI in in the last column represents color rendering index.

Device	V_{on} (V)	PE (lm/W) max/1000/5000[a]	CE (cd/A) max/1000/5000[a]	EQE (%) max/1000/5000[a]	CIE 1000[b]	CRI 1000[b]
0.02 nm	2.7	59.2/48.4/36.7	55.3/52.9/46.8	22.3/21.3/19.2	0.31,0.40	63
0.04 nm	2.7	63.2/53.4/40.3	59.3/57.1/50.4	23.1/22.2/19.9	0.35,0.42	65
0.06 nm	2.7	63.4/53.6/38.7	59.7/57.6/51.1	22.4/21.6/19.5	0.41,0.41	62
0.08 nm	2.7	64.8/55.1/41.2	61.1/59.1/52.0	22.3/22.0/19.6	0.42,0.45	60

[a]The maximum efficiency/the efficiency at 1000 cd/m^2/the efficiency at 5000 cd/m^2.
[b]At the luminance of 1000 cd/m^2.

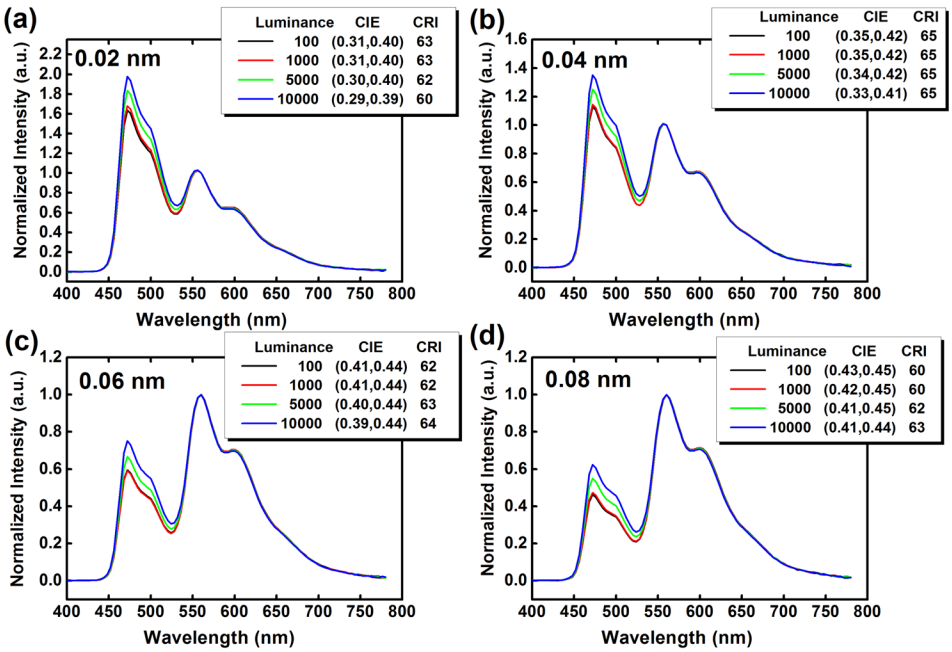

FIG. 3. Normalized EL spectra of the four WOLEDs at the luminance from 100 cd/m^2 to 10000 cd/m^2.

and 26DCzPPy:FIrpic layers, and the orange emission intensity is gradually decreased with the thin orange layer far from the middle interface. This means that the exciton recombination zone should be in the middle range of EML, as shown in Figure 4, from 2 nm in TCTA:FIrpic layer to 3 nm in 26DCzPPy:FIrpic, and the exciton density should also be the maximum at the interface, showing approximate Gaussian distribution. This kind of effective exciton density profile greatly increases the exciton recombination efficiency and significantly reduces the exciton quenching caused by the exciton diffusion into transport layers. This can also be used to explain the reason why using a very thin orange emission layer in EML can obtain a strong orange emission, too. The exciton recombination zone contribution may also be well explained by the energy levels and transport properties of TCTA and 26DCzPPy. As we know, TCTA is a good hole transport organic material with mobility of 3×10^{-4} cm^2/V s (electron mobility is about 10^{-8} cm^2/V s),[24] and 26DCzPPy is a good bipolar transport organic molecule with equivalent

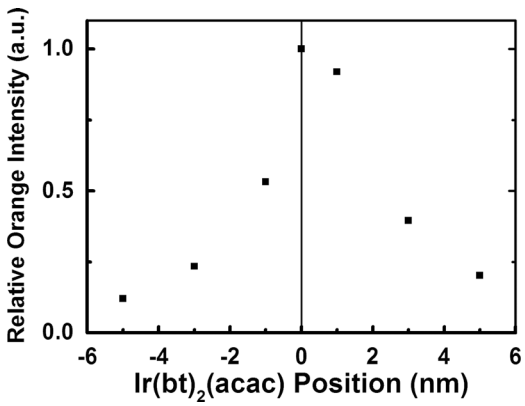

FIG. 4. Relative orange emission intensity in OLEDs by inserting an ultra-thin orange layer at the different positions in EML. The applied voltage is 3.9 V. The middle position between TCTA:FIrpic and 26DCzPPy:FIrpic layers is set as 0 nm.

electron and hole mobility of 2×10^{-5} cm^2/V s.[25] Therefore, according to the energy levels of TCTA (LUMO = 2.43 eV, HOMO = 5.83 eV) and 26DCzPPy (LUMO = 2.56 eV, HOMO = 6.05 eV), as shown Figure 1(c), the holes from anode easily transport along the HOMO of TCTA to the interface of TCTA/26DCzPPy, and then the parts are injected into the HOMO of 26DCzPPy by a barrier of about 0.2 eV and transport along 26DCzPPy molecules due to its good hole transport property. Similarly, the electrons from cathode first transport along the LUMO of 26DCzPPy and easily arrive at the interface of TCTA/26DCzPPy due to the good electron transport property of 26DCzPPy. Because of the electron injection barrier of 0.13 eV and poor electron transport property of TCTA, few electrons at interface will transport into TCTA layer and most of them will accumulate at the thin region of TCTA layer adjacent to the interface. Evidently, this electron and hole contribution in EML also leads to a narrower exciton recombination zone in TCTA:FIrpic layer than in 26DCzPPy:FIrpic layer.

To fully understand the EL processes of the resulting WOLEDs based on an ultra-thin orange emission layer, we further studied the EL mechanism of orange emission from Ir(bt)$_2$(acac) in EML. As we know, in doped OLEDs, host-guest energy transfer and direct charge trapping followed by exciton formation on dopants are two main emission mechanisms. A distinction between the two emission mechanisms can be drawn from the dependence of current density-voltage (J-V) on guest concentration. For the direct charge trapping process, the dopant molecules may be considered as shallow trapping centers, which will trap the injected charge carriers and change the charge density, resulting in a dependence of J-V characteristics on the doping concentration. For the energy transfer counterpart, however, the J-V characteristics are not influenced by the variation of the doping concentration. From the energy levels of the device in Figure 1(c), we can see that the HOMO and LUMO levels of Ir(bt)$_2$(acac) are within those of TCTA, FIrpic, and 26DCzPPy. This means

that the $Ir(bt)_2(acac)$ orange emission in EL may include the charge carrier trapping process. To elucidate this point, we fabricated OLEDs with orange layer thickness from 0 nm to 0.2 nm, which is similar to increasing the $Ir(bt)_2(acac)$ concentration in host. Figure 5 shows the *J-V* characteristics of the devices. The inset of Figure 5 gives the double logarithmic plot. It is clearly seen that the *J-V* characteristics do not change with the $Ir(bt)_2(acac)$ thickness, implying that the primary emission mechanism of $Ir(bt)_2(acac)$ in EL is actually the energy transfer process rather than the carrier trapping effect.

Considering the T_1 level of the involved hosts and guests, the exothermic energy transfer from higher T_1 of TCTA, 26DCzPPy, and FIrpic to lower T_1 of $Ir(bt)_2(acac)$ is reasonable. There have been reports about the exciton lifetime change in energy transfer process.[12,15] The lifetime of the donor will decrease if the energy transfer process from the donor to the acceptor happens. Here, we examined the transient EL characteristics of two devices with (white device) or without (blue device) a 0.06 nm orange $Ir(bt)_2(acac)$ layer. Figure 6 displays the transient EL spectra of the two devices monitored at a wavelength of 472 nm. The lifetime of blue device is fitted to be 1.74 μs (τ_1), and the lifetime of white device is decreased to 1.34 μs (τ_2). The lifetime of triplets in the blue device can be expressed as follows if triplet-triplet annihilation (TTA) is not considered:

$$\tau_1 = 1/(\kappa_R + \kappa_{NR}). \quad (1)$$

Here, κ_R and κ_{NR} are the rate constants of the radiative and non-radiative processes. While in the white device, the energy transfer from FIrpic to $Ir(bt)_2(acac)$ has to be considered, then the lifetime of the triplets on FIrpic should be

$$\tau_2 = 1/(\kappa_R + \kappa_{NR} + \kappa_{ET}), \quad (2)$$

where κ_{ET} is the rate constant of the energy transfer from FIrpic to $Ir(bt)_2(acac)$. Then, we can derive the energy transfer efficiency from Eqs. (1) and (2)

$$\eta_{ET} = \kappa_{ET}/(\kappa_R + \kappa_{NR} + \kappa_{ET}) = 1 - \tau_2/\tau_1 = 23.0\%, \quad (3)$$

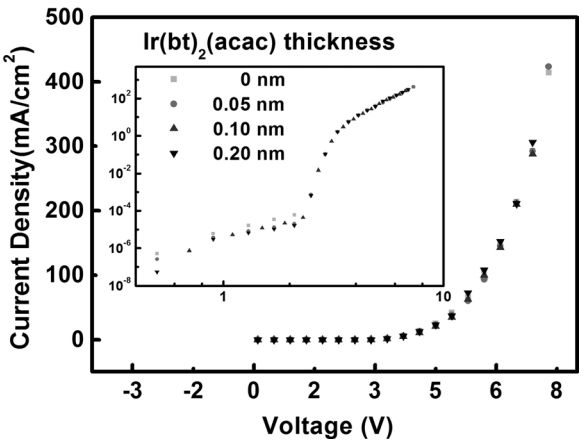

FIG. 5. Current density-voltage dependence of the devices with $Ir(bt)_2(acac)$ thickness from 0 nm to 0.2 nm. The inset gives double logarithmic curves of the devices.

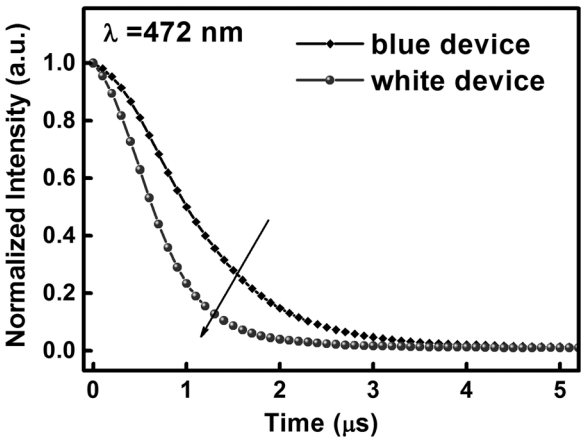

FIG. 6. Transient EL signals of devices without (blue device (diamond)) and with (white device (ball)) 0.06 nm $Ir(bt)_2(acac)$ layer. The driving voltage is 4 V.

where η_{ET} is the energy transfer ratio from the donor to the acceptor. It can be seen that there indeed exists an energy transfer process in $Ir(bt)_2(acac)$ EL process, and if including the energy transfer from the excitons on TCTA and 26DCzPPy, obviously the energy transfer is very efficient, leading to a strong $Ir(bt)_2(acac)$ orange emission.

As shown in Figure 2, although the efficiency roll-off of the resulting WOLEDs here is greatly improved, the roll-off yet exists at higher luminance. The critical current density J_0 is defined as the point where the quantum efficiency is reduced to half its maximum value, which is proposed by Baldo *et al.*[26] In order to figure out the cause of efficiency roll-off in our devices, we apply the models of TTA and triplet-polaron quenching (TPQ) to the interpretation of the high current density performance of our blue and white devices.[6,26] When TTA happens, the reaction between triplet excitons follows:

$$^3M^* + {}^3M^* \xrightarrow{k_{TT}^S} {}^1M^* + M, \quad (4)$$

$$^3M^* + {}^3M^* \xrightarrow{k_{TT}^T} {}^3M^* + M, \quad (5)$$

where $^3M^*$ represents triplet excited state, $^1M^*$ is the singlet excited state, M is the ground state, and k_{TT} is the TTA rate parameter for singlet and triplet exciton. Then the concentration of triplet excited state can be expressed as

$$\frac{d[^3M^*]}{dt} = \frac{[^3M^*]}{\tau} = \frac{k_{TT}}{2}[^3M^*]^2 + \frac{J}{qd}, \quad (6)$$

where J is the current density, q is the charge density, d is the thickness of the carrier recombination zone, and τ is the phosphorescence lifetime. In addition, J/qd is the charge density in the RZ.

For TPQ process, the quenching is described as

$$M^+(\text{or } M^-) + {}^3M^* \xrightarrow{K_e} M^+(\text{or } M^-) + M, \quad (7)$$

where M^+(or M^-) is the trapped charge carriers assumed to annihilate the triplet excitons and k_e is the TPQ rate parameter. Then this process can be expressed as

$$\frac{d[^3M^*]}{dt} = \frac{[^3M^*]}{\tau} = k_e[^3M^*]n_t + \frac{J}{qd}, \tag{8}$$

where n_t represents the concentration of the trapped charge carrier. Based on trap limited space charge conduction,[27] $n_t \sim J^{l/(1+m)}$, then equation follows:

$$\frac{d[^3M^*]}{dt} = \frac{[^3M^*]}{\tau} = -k_e[^3M^*]\mathbf{J}^{1/(m+1)} + \frac{J}{qd}. \tag{9}$$

From Eqs. (6) and (9), we can see that when the quenching is TTA predominant, the quenching should increase quadratically with the triplet exciton density while the TPQ predominant process should increase linearly with the triplet exciton density. The current density dependence of the EQE in both models can be derived from Eqs. (6) and (9) and gives, respectively,

$$\frac{\eta_{TT}}{\eta_0} = \frac{J_0}{4J}\left[\sqrt{1+8\frac{J}{J_0}} - 1\right], \tag{10}$$

$$\frac{\eta_{PT}}{\eta_0} = \frac{1}{1+\left(\frac{J}{J_e}\right)^{m+1}}, \tag{11}$$

where η_0 is the external quantum efficiency in the absence of triplet quenching, η_{TT} is in the presence of TTA, η_{PT} is in the presence of TPQ, and J_0 and J_e are the critical current density for TTA and TPQ models. Among

$$J_0 = \frac{4qd}{\tau^2 k_{TT}}, \tag{12}$$

$$J_e = \left(\frac{1}{k_e\tau}\right)^{m+1}. \tag{13}$$

Then, we apply Eqs. (10) and (11) to our blue and white devices. As shown in Figure 7, it can be seen that the TTA model presents a good agreement with our devices while the TPQ model cannot fit well. By TTA model fitting, $J_0 = 150.3\,\mathrm{mA/cm^2}$ and $120.5\,\mathrm{mA/cm^2}$, respectively, for white and blue devices, are obtained. The above results indicate that the roll-off in efficiency of our WOLEDs at high luminance is primarily due to the TTA. Although the efficiency roll-off at higher brightness yet exists in our devices, however, as given, the achievement of high J_0 is over $150\,\mathrm{mA/cm^2}$, which is higher than most of the previously reported value in WOLEDs including all-phosphorescent[15,22] and hybrid WOLEDs,[28] indicates that the utilization of the ultra-thin orange emission layer in our devices is still benefitted to eliminate the TTA, thus improving the roll-off in efficiency at high brightness.

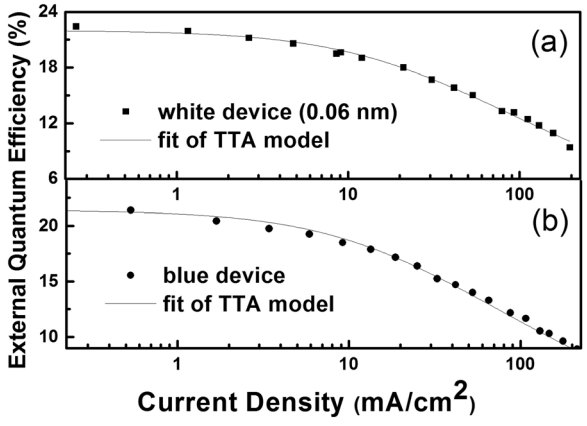

FIG. 7. External quantum efficiency vs current density of white device (a) and blue device (b). The corresponding fitting curves based on the TTA model are also shown (solid lines).

IV. CONCLUSIONS

We have demonstrated highly efficient phosphorescent WOLEDs by simply introducing an ultra-thin non-doped orange emission layer in EML. The WOLEDs exhibit a maximum power efficiency of 63.2 lm/W, current efficiency of 59.3 cd/A, and EQE of 23.1%, which are slightly reduced to 53.4 lm/W, 57.1 cd/A, and 22.2% at $1000\,\mathrm{cd/m^2}$, respectively, showing greatly improved roll-off in efficiency. Our results demonstrate that ultra-thin non-doped emissive layer method on constructing high efficiency WOLEDs is very effective and cost-saved. This research provides a simple strategy in the design of high efficient WOLED device and with the use of out-coupling techniques, the performance of the device will be greatly enhanced.

ACKNOWLEDGMENTS

The authors gratefully acknowledge the National Natural Science Foundation of China (51333007 and 50973104), Ministry of Science and Technology of China (973 Program No. 2013CB834805), the Foundation of Jilin Research Council (2012ZDGG001, 20130206003GX, and 201105028), and CAS Instrument Project (YZ201103) for the support of this research.

[1]M. A. Baldo, D. F. O'Brien, Y. You, A. Shoustikov, S. Sibley, M. E. Thompson, and S. R. Forrest, Nature **395**, 151 (1998).
[2]M. Ikai, S. Tokito, Y. Sakamoto, T. Suzuki, and Y. Taga, Appl. Phys. Lett. **79**, 156 (2001).
[3]Y. Sun and S. R. Forrest, Appl. Phys. Lett. **91**, 263503 (2007).
[4]Y.-L. Chang, Y. Song, Z. Wang, M. G. Helander, J. Qiu, L. Chai, Z. Liu, G. D. Scholes, and Z. Lu, Adv. Funct. Mater. **23**, 705 (2013).
[5]Z. B. Wang, M. G. Helander, J. Qiu, D. P. Puzzo, M. T. Greiner, Z. M. Hudson, S. Wang, Z. W. Liu, and Z. H. Lu, Nat. Photonics **5**, 753 (2011).
[6]C. Adachi, M. A. Baldo, M. E. Thompson, and S. R. Forrest, J. Appl. Phys. **90**, 5048 (2001).
[7]Y. Sun, N. C. Giebink, H. Kanno, B. Ma, M. E. Thompson, and S. R. Forrest, Nature **440**, 908 (2006).
[8]Y. Sun and S. R. Forrest, Org. Electron. **9**, 994 (2008).
[9]Q. Wang, J. Ding, D. Ma, Y. Cheng, L. Wang, and F. Wang, Adv. Mater. **21**, 2397 (2009).
[10]S. Reineke, F. Lindner, G. Schwartz, N. Seidler, K. Walzer, B. Lussem, and K. Leo, Nature **459**, 234 (2009).
[11]H. Sasabe, J.-i. Takamatsu, T. Motoyama, S. Watanabe, G. Wagenblast, N. Langer, O. Molt, E. Fuchs, C. Lennartz, and J. Kido, Adv. Mater. **22**, 5003 (2010).
[12]Y. Zhao, L. Zhu, J. Chen, and D. Ma, Org. Electron. **13**, 1340 (2012).
[13]Q. Wang, J. Ding, D. Ma, Y. Cheng, L. Wang, X. Jing, and F. Wang, Adv. Funct. Mater. **19**, 84 (2009).
[14]Q. Wang and D. Ma, Chem. Soc. Rev. **39**, 2387 (2010).
[15]B. W. D'Andrade, R. J. Holmes, and S. R. Forrest, Adv. Mater. **16**, 624 (2004).
[16]H. Yang, Y. Zhao, W. Xie, Y. Shi, W. Hu, Y. Meng, J. Hou, and S. Liu, Semicond. Sci. Technol. **21**, 1447 (2006).
[17]Z. Su, W. Li, M. Xu, T. Li, D. Wang, W. Su, J. Niu, H. He, J. Zhu, and B. Chu, J. Phys. D: Appl. Phys. **40**, 2783 (2007).

[18]S. Chen, Z. Zhao, B. Z. Tang, and H. S. Kwok, J. Phys. D: Appl. Phys. **43**, 095101 (2010).
[19]Y. Zhao, J. Chen, and D. Ma, Appl. Phys. Lett. **99**, 163303 (2011).
[20]Y. Zhao, J. Chen, and D. Ma, ACS Appl. Mater. Interfaces **5**, 965 (2013).
[21]M.-T. Lee, M.-T. Chu, J.-S. Lin, and M.-R. Tseng, J. Phys. D: Appl. Phys. **43**, 442003 (2010).
[22]S. J. Su, E. Gonmori, H. Sasabe, and J. Kido, Adv. Mater. **20**, 4189 (2008).
[23]G. Schwartz, M. Pfeiffer, S. Reineke, K. Walzer, and K. Leo, Adv. Mater. **19**, 3672 (2007).
[24]J.-W. Kang, S.-H. Lee, H.-D. Park, W.-I. Jeong, K.-M. Yoo, Y.-S. Park, and J.-J. Kim, Appl. Phys. Lett. **90**, 223508 (2007).
[25]C. Cai, S.-J. Su, T. Chiba, H. Sasabe, Y.-J. Pu, K. Nakayama, and J. Kido, Org. Electron. **12**, 843 (2011).
[26]M. A. Baldo, C. Adachi, and S. R. Forrest, Phys. Rev. B **62**, 10967 (2000).
[27]M. A. Lampert and P. Mark, *Current Injection in Solids* (Academic Press, New York, 1970).
[28]N. Sun, Q. Wang, Y. Zhao, Y. Chen, D. Yang, F. Zhao, J. Chen, and D. Ma, Adv. Mater. **26**, 1617 (2014).